

The paraglacial adjustment of an Alpine lateral moraine, Bas Glacier d’Arolla, Switzerland

Toby N. Tonkin

Faculty of Arts, Science, and Technology, University of Northampton, University Drive, Northampton, UK.

ABSTRACT

Within Alpine catchments, glacial landforms are subject to post-depositional reworking during and following deglaciation. Ice-marginal moraines are thought to rapidly stabilise within ~200 years in this topographic context, although ice-proximal slopes are particularly prone to alteration by debris flows and solifluction. This study investigates landform transformation, documenting geomorphological change at the Bas Glacier d’Arolla, Switzerland. Gully development on a moraine slope was assessed using archive image sets obtained in 1977, 1988 and 2009 to derive historical elevation models. Raster differencing suggests that the mean rate of surface lowering on the upper moraine slope was 7.15 ± 1.83 m (\pm minimum level of detection) over the observation period (1977–2009), a rate of 0.22 m yr⁻¹. The erosion of the landform resulted in an incontinuous moraine crestline. Whilst some landforms may undergo limited transformation upon deglaciation, selected sites are subject to rapid geomorphologic change, involving crestline retreat via the initial dissection by gullies, followed by the removal of inter-gully slopes.

DOI: [10.1080/02723646.2023.2212989](https://doi.org/10.1080/02723646.2023.2212989)

Introduction

Large lateral moraines develop following the repeated reoccupation of mountain valleys by glacier ice (Lukas *et al.*, 2012; Röthlisberger & Schneebeli, 1979). These landforms are characterised by their large size, attaining a topographic prominence of up to ~100 metres, sharp moraine crestlines, and an asymmetric form. Debris transfer via falls, slumps, slides and flowage (“dumping”) is regarded as an important mechanism for the formation of Alpine-type lateral moraines (Benn *et al.*, 2003; Small, 1983), and moraine formation is conventionally associated with sediment transfer from a supraglacial to an ice-marginal position (Humlum, 1978). Moraine formation may be topographically controlled (Barr & Lovell, 2014), resulting in either the accretion or superposition of diamicton onto ice-proximal or distal slopes (Röthlisberger & Schneebeli, 1979). Moraine building may also be episodic, with interrupted periods of moraine construction via superimposition, resulting in the preservation of organic materials such as palaeosols. Such material can be used to derive a minimum age for glacier recession and maximum ages for renewed moraine construction and thus glacier advance (Kirkbride & Winkler, 2012).

Following glacier recession, the removal of glacier-support leaves ice-proximal slopes susceptible to paraglacial reworking (Ballantyne, 2002). Moraines in alpine settings often have a distinctive morphology characterised by over-steepened ice-proximal slopes that are reported to locally approach 80° (Lukas *et al.*, 2012). These ice-proximal slopes are known to remain in a quasi-stable state. Clast macrofabrics in lateral moraines may dip away from the former glacier surface, and this has been linked to inherent landform stability (Curry *et al.*, 2009). Ice-proximal slope stability has also been attributed to the presence of over-consolidated/compacted or “plastered on” diamicton, where exceptionally strongly clustered clast macrofabrics parallel to ice flow have been interpreted as evidence of the incremental plastering (“lodgement”) of primarily subglacial till on to ice-proximal moraine slopes (Lukas *et al.*, 2012).

Despite this apparent stability, geomorphological change during deglaciation results in the reworking of moraines and sediment-mantled slopes (Ballantyne, 2002). Studies have sought to understand landform stability and the paraglacial response of moraines during deglaciation. Curry *et al.* (2006) observed paraglacial processes operating on moraines and sediment-mantled slopes in the Swiss Alps, reporting minimum average erosion rates of 0.095 m yr^{-1} , with moraine slopes found to stabilise within 80–140 years following deglaciation. Similarly, a study in western Norway found that rates of lowering may range between 0.05 and 0.1 m yr^{-1} (Benn and Ballantyne, 1994). Debris from gullied moraine slopes can be a source of supraglacial sediment, influencing the ablation of glacier surfaces; however, further work quantifying the significance of this negative feedback is suggested to be required (van Woerkom *et al.*, 2019).

Advances in geospatial methods such as Structure-from-Motion photogrammetry (Mertes *et al.*, 2017; Westoby *et al.*, 2012) and ground-based Light Detection and Ranging (LiDAR) have provided opportunities to better understand the rates of landform transformation. For example, a multi-method remote sensing study by Dusik *et al.* (2019) used multitemporal Digital Elevation Models (DEMs) to study the intra- and interannual erosion of a Little Ice Age moraine. The authors found that extreme summer events played an important role in sediment mobilisation. A longer-term study by Betz-Nutz *et al.* (2023) used archival aerial images from the 1950s to document decadal scale change at multiple glacier forelands. Rates of landform transformation were found to slow over time, but critically, where initial rates of change were high, erosion did not decline over time as previously hypothesised (Betz-Nutz *et al.*, 2023). Further complexity in the process of moraine stabilisation relates to the interplay of biogeomorphologic thresholds (Draebing & Eichel, 2018), vegetation colonisation and disturbance (Eichel, 2019). The role of engineer species such as *Dryas octopetala* in promoting a switch from debris flows and slides to bound solifluction has been recognised (Eichel *et al.*, 2016), with the authors introducing the concept of the “biogeomorphologic feedback window”.

Our understanding of (para)glacial processes have been improved using archival imagery and change detection approaches in other sub-sets of the glaciated valley landsystem (e.g. Bennett & Evans, 2012; Schiefer & Gilbert, 2007). Gully erosion and moraine lowering in Alpine settings is less well documented in the literature in comparison to high-Arctic landforms, and a better understanding of moraine degradation via external censoring is of interest to Quaternary scientists seeking to understand glacier response via the interpretation of radiometric dates obtained from these landforms (Tomkins *et al.*, 2021; Heyman *et al.*, 2011; Putkonen & Swanson, 2003;). This study investigates the stability and transformation of Alpine lateral moraines using archive image sets. The objectives are threefold: (1) to derive rates of landform transformation in a valley glacier landsystem; (2) to investigate changes in the rate of change during a period of deglaciation; and (3) discuss the implications of geomorphologic change in relation to the reconstruction of Alpine glacier activity.

Study site

The Bas Glacier d’Arolla is located at the base of Mont Collon (~3636 m; Datum = LN02) in the Valais area of Switzerland. The glacier has a predominantly northern aspect and drains into the western branch of the Val d’Herons (Borgne d’Arolla). Goodsell *et al.* (2002) highlight that the Bas Glacier d’Arolla was named *c.* 1949, following disconnection from Glacier du Mont Collon, located to the south-west and Haut Glacier d’Arolla to the south-east (Figure 1). For this reason, the Bas Glacier d’Arolla is now avalanche fed from the north-facing flank of Mont Collon.

The Bas Glacier d’Arolla has been subject to previous geomorphological and glaciological investigations, including studies with a focus on proglacial channel development (Warburton & Fenn, 1994; Warburton, 1994), glacier flow and ogive formation (Goodsell *et al.*, 2002; Haefeli, 1951), and glacier erosion (Warburton & Beecroft, 1993). The Val d’Herons experienced a mean annual precipitation of 720 mm between 1987 and 2012 (Lambiel *et al.*, 2016). Between 1856 and 2020

the glacier receded by ~1.4 km (GLAMOS, 2022). This overall pattern of recession was punctuated by a ~140 m glacier advance between ca. 1971 and 1987. The Little Ice-Age maximum extent of the Bas Glacier d’Arolla is demarcated by a prominent (~150 m in elevation) moraine. Colonisation has occurred in the latero-frontal section of this landform; however, the section analysed in this study is largely unvegetated. Previous investigators note that the lateral moraine is set against the valley side, has in-excess of 40 gullies per kilometre on the ice-proximal slope, and has an average crestline altitude of ~2150 m (Curry *et al.*, 2006). At this site slopes locally exceed 60°, however, rates of landform denudation at the site are currently unknown. Furthermore, the longer-term pattern of glacier activity at Bas Glacier d’Arolla over the Holocene is unclear. Long-term glacier activity has been documented at the nearby Tsidjoire Nouve; a glacier also draining into the western branch of the Val d’Herons ~4 km from the study site. Here, Terrestrial Cosmogenic Nuclide dating (¹⁰Be) of moraine deposits has revealed the occupation of ice in Val d’Herons by ~11.4 ka, and provide evidence for a subsequent Holocene advance ~3.8 ka before 2010 CE (Schimmelpfennig *et al.*, 2012). At the Bas Glacier d’Arolla, moraine morphology reflects the Little Ice Age advance of ice into the valley.

Methods

Target imagery

Between four and six images were selected from each dataset for image processing. All images fully or partially contained the 2.5 km² landform of interest, with photography captured along a single flight line with onlap often exceeding 75%. All the images were taken using black and white film cameras as contact prints (originally 23 × 23 cm) and were digitally scanned by the Swiss Federal Office of Topography (SwissTopo). The scanned images from 1977 ($n = 4$), 1988 ($n = 6$), and 2009 ($n = 4$) were provided in tagged image format alongside any known metadata. Other image sets from 1961, 1964, 1965, 1967, and 1983 were also considered for analysis; however, the resulting point clouds had excessive noise, artefacts, or gaps

within the area of interest. Depth filtering, image contrast enhancement, and the removal of blurred imagery, were trialled to help resolve the geometry of the lateral moraine. Due to the subtle topographic change associated with moraine degradation – a focus of this study – these image sets were considered less-suitable for further image processing and subsequently omitted from the analysis.

Image processing

The image processing was conducted in Agisoft Metashape (ver. 1.8.4) using established workflows for the generation of elevation data from archival image sources (e.g. Midgley & Tonkin, 2017; Mölg and Bolch, 2017; Mertes *et al.*, 2017). Specifically, this involved: (1) fiducial marker identification; (2) image masking to remove the image frame; (3) sequential image alignment and sparse cloud generation; (4) georeferencing via a series of off-glacier ground control points with known positions that surround the target landform; (5) camera self-calibration and optimisation; and (6) dense cloud production with moderate depth filtering. Where camera orientation metadata were unavailable, self-calibrated camera models, where internal (e.g. radial distortion and focal length) and external (camera position and pose) parameters are estimated, were used. Critically, where calibration metadata are unavailable, self-calibration is known to produce robust topographic data deriving estimates of long-term elevation change (Mertes *et al.*, 2017). However, this is contingent on the use of an appropriate ground-control network (James *et al.*, 2017).

Georeferencing and DEM generation

Similar to the approach of Mölg and Bolch (2017) and Mannerfelt *et al.* (2023), who also generate elevation data from archival imagery using photogrammetry, existing elevation and image datasets were used to georeference derived data from the 1977, 1988, and 2009 image sets. To ensure the relative accuracy of the three photogrammetrically derived point clouds, all were georeferenced to the most recent SwissALTI^{3D} data product. The SwissALTI^{3D} elevation model was produced using stereo-correlation with an altimeter accuracy of 1–3 m for areas above 2000 m

(SwissTopo, 2019). The data have a 0.5 m spatial resolution and are referenced using the CH1903+/LV95 coordinate system (EPSG:2056). The SwissALTI^{3D} DEM was used in combination with the SwissImage orthophoto which is available at a spatial resolution of 0.1 m. The orthorectified imagery – acquired in 2020 – is reported to have a planimetric accuracy of ± 0.1 m (1 sigma errors) in the area of interest. These data are not assumed to be error free but, as the purpose of this investigation is to estimate landform evolution, it is the *relative* accuracy, opposed to the absolute accuracy that is important. Eight off-glacier boulders located on stable terrain around the glacier margin were used as ground-control points for the purpose of georeferencing the respective dense point clouds generated by this study. To reduce uncertainty in the derived data the same eight markers were used as ground-control points in the 2009, 1988, and 1977 image sets, with reported RMS errors of 1.05, 1.80, and 1.49 pixels respectively. Images were matched using the highest quality parameter setting and sequential selection.

A clipped area of interest containing the landform was represented in dense point clouds with ~ 12 , ~ 10 , and ~ 3 million points, with average point densities of 7.13, 7.8 and 1.74 points per m^2 for the 1977, 1988 and 2009 data, respectively. The resulting DEMs were rasterised from the raw dense point clouds in CloudCompare (ver. 2.12.4). Here, georeferenced 2 m spatially concurrent and orthogonal DEMs were generated using linear interpolation with cells representing the average elevation value within the cell footprint as calculated from the respective z-values stored within the dense point clouds.

Quality assessment

Two Emlid Reach RS+ GNSS (Global Navigation Satellite System) receivers were used to obtain coordinates for off-glacier locations on stable terrain to aid understanding of the vertical accuracy of the SwissAlti^{3D} DEM in the area of interest. Static positioning, where a receiver occupied four fixed points for between ~ 2 and ~ 5 hours was used to obtain positions. The absolute accuracy of these data

was improved using a Post-Processing Kinematic (PPK) solution obtained from a continuously operating reference base station (CORS) located in Lignan, Italy (ID: LIGN00ITA). These data, provided via the EUREF Permanent Network, were available for the duration of the GNSS survey in RINEX V3.03 format, providing a survey baseline of ~23 km. The post-processing was conducted using Emlid Studio (ver. 10.14). The corrected survey points were used to calculate the vertical RMS (Root-mean-square) error of occupied fixed points on the SwissAlti^{3D} DEM. This confirmed the absolute accuracy of the SwissAlti^{3D} DEM to within the suggested 1–3 m range (RMS error = 2.94 m).

To assess the relative accuracy of the derived DEMs, a total of 30,624 off-glacier, and spatially coincident cells, on stable and partially vegetated terrain were used to assess uncertainty in these data. Comparisons between these data points and the 1977–1988, 1988–2009 and 1977–2009 epochs yielded mean differences of -0.17 ± 0.98 , 0.06 ± 1.07 , and -0.11 ± 0.57 m (\pm the standard deviation of errors), respectively. The median vertical differences were equal to or within ± 1 decimetre for all epochs. Further assessment of the relative accuracy of these data was achieved using the spatially concurrent DEMs (1977, 1988, and 2009) and a two-metre spatial resolution upscaled version of the 2019 SwissAlti^{3D} data product generated with the SAGA GIS (ver. 7.3.0) (Conrad *et al.*, 2015) resampling tool using a cell-weighted mean-value. For the same 30,624 cells, the standard deviation of the vertical error was found to be 0.79 m (σ_{1997}), 1.13 m (σ_{1988}), and 0.51 m (σ_{2009}). For the 2009 and 1977 datasets >95% of cells on stable terrain were within ± 1.5 m of the SwissAlti^{3D} data. Overall, the relative accuracy of the spatially concurrent DEMs was found to be acceptable for the purpose of detecting metre-magnitude geomorphological change over a decadal timescale, given the scale of the target imagery (Micheletti *et al.*, 2015).

Assessment of surface change

The generation of concurrent and orthogonal DEMs enabled changes in surface elevation (z-axis) to be derived using raster differencing. This technique is well

suites for the detection of change in glacial landscapes (Chandler *et al.*, 2020; Cody *et al.*, 2020; Tonkin *et al.*, 2016). To ensure confidence in the change detection results, the approach of Brasington *et al.* (2003) was used to filter cells that fell below the estimated minimum level of detection (LoD) at the specified confidence interval under a normal distribution (t) (equation below).

$$LoD = t (\sigma_{z1}^2 + \sigma_{z2}^2)^{\frac{1}{2}}$$

Here the standard deviation (σ) of the vertical differences (stable terrain) between the photogrammetrically derived DEMs and reference SwissAlti^{3D} DEM is used. For this study, Digital Elevation Models of Difference (DoD) were calculated using a 95% confidence interval ($t = 1.96$). Raster differencing was undertaken using the standalone version of the Geomorphological Change Detection toolset (Wheaton *et al.*, 2010; ver. 7.5.0). A subset of spatially coincident cells on remnant moraine sections (referred hereafter as “inter-gully slopes”, after Curry *et al.*, 2006) were sampled from a topographic profile across the upper ice-proximal slope of the landform (Figure 2). The same process was used to sample a subset of cells from gullied sections of the moraine bounded by these inter-gully slopes for the purpose of understanding differences in the rate of change in these respective landform elements (Figure 2). These data were subject to inferential tests of difference using a Student’s t -test in Minitab®. The rate of surface transformation from two epochs (E_1 and E_2) was also compared using a paired-sample t -test.

As these raster differences yield surface elevation change in the z dimension, cloud-to-cloud differencing (C2C) was also undertaken as a second measure of moraine surface adjustment over the observation period (E_d). The advantage of point-cloud-based change detection is that it circumvents the need for rasterisation – a potential source of error in topographic data (Midgley & Tonkin, 2017). The closest point distance (L_{C2C}) represents the Euclidean length between a point in the reference cloud and its nearest neighbour in the comparison cloud (Winiwarter *et al.*, 2021; Lague *et al.*, 2013). This approach yields absolute values of distance that are not directionally signed (DiFrancesco *et al.*, 2020) and is therefore used to compliment

the assessment of gully erosion (lowering) over the observation period offering insight into both the horizontal and vertical components of moraine slope adjustment.

Results

Calculations yielded LoD₉₅ values of 2.71 m for the 1977–1988 epoch (E_1), 2.43 m for the 1988–2009 epoch (E_2), and 1.83 m for the 1977–2009 epoch (E_d). These values provide an appropriate and reasonable level of detection in comparison with an earlier digital photogrammetric study in the Arolla area, where due to the scale of the archival imagery available, only metre magnitude changes were reliably detected (Micheletti *et al.*, 2015). Change exceeded LoD₉₅ for 45.4%, 53.0%, and 52.7% of the area of interest for E_1 , E_2 , and E_d , respectively, with the pattern of change concentrated around areas of glacier change, and on exposed ice-proximal slopes undergoing paraglacial gullying (Figures 2 and 3). Notably, the pattern of glacier advance and retreat is evident on the DEM of Difference and cloud-to-cloud differencing, corresponding with the formation of a small inset moraine on the true left lateral moraine. Over the entire observation period (E_d), the upper moraine slope zone (Figure 3) was found to have an average depth of surface lowering of 7.15 ± 1.83 m (thresholded) corresponding to the removal of in excess of $1.56 \times 10^5 \pm 0.39 \times 10^5$ m³ of diamicton. Beneath this landform zone, the presence of an ice-cored supraglacial lateral moraine throughout the observation period was noted; however, rapid degradation by 2009 was evident in the image sets analysed and associated DEMs of Difference (Figure 3).

A paired *t*-test found a significant difference in the yearly rate of vertical incision in well-developed gullies between E_1 and E_2 ($t_{(25)} = -5.25$; $p < .001$), with average rates of change reducing from 0.26 ± 0.18 to 0.05 ± 0.08 m yr⁻¹ (± 1 SD). The inter-gully slopes also experienced a statistically significant reduction in the vertical rate of landform transformation between epochs ($t_{(25)} = -5.20$; $p < .001$), with the average rate of change of 0.53 ± 0.24 and 0.19 ± 0.13 m yr⁻¹ in E_1 and E_2 , respectively (Figures 4 and 5).

When the rates of surface transformation over the entire duration of the observation period (E_d) on gullies and the associated inter-gully slopes were compared, a two-sample t -test found a significant difference in the average rate of surface lowering between these landform elements ($t_{(49)} = 9.28, p < .001$). Inter-gully slopes, on average, experienced higher rates of vertical change over the observation period than the gullies (Figures 4 and 5). Lower ice-proximal slopes tended to fall within the minimum Level of Detection (LoD_{95}) (Figure 4). When mapped in planform, the moraine crestlines were found to have retreated between 7.2 and 15.8 m (Mean = 11.1) over E_d . This corresponds to an average rate of moraine crestline retreat of $\sim 0.35 \text{ m yr}^{-1}$. Two sections of the previously contiguous moraine crestline eroded to bedrock as a consequence of encroaching gullies during the observation period (Figure 3). Finally, absolute differences between clouds (L_{C2C}) yield average values of $4.22 \pm 2.73 \text{ m}$ (1 SD) for the gullied upper moraine slopes (a total of 454,422 L_{C2C} values) with 75.7% of L_{C2C} distances found to exceed 2 m (Figure 4).

Discussion

Rates of landform transformation

At the Bas Glacier d'Arolla the rate of moraine crestline retreat was found to average $\sim 0.35 \text{ m yr}^{-1}$. Over the observation period, this rate of landform transformation resulted in the removal of a once contiguous moraine crestline associated with the Little Ice Age glacier advance. There is, however, a paucity of rates of planimetric crestline change available for comparison in the wider literature, and further work in mountain environments utilising archive imagery as a baseline would help contextualise the significance of this finding. Previous studies have, however, demonstrated that high rates of lateral moraine crestline retreat can be linked to slope instability – particularly landslide activity (Blair, 1994; Lukas *et al.*, 2012) – which may significantly alter moraine crestlines by tens of metres (Betz-Nutz *et al.*, 2023). At Bas Glacier d'Arolla there is no evidence of large-scale failure, with the high rates of change more likely associated with the known processes of paraglacial moraine degradation (Ballantyne & Benn, 1994): the

wasting of inter-gully slopes by sliding and debris falls, concentrated on the sidewalls, and the subsequent removal of sediment by debris flows onto the lower moraine slopes (Curry *et al.*, 2009). This study therefore highlights that landslide activity on moraine slopes may not be the only process responsible for high rates of geomorphological change during deglaciation.

The current study also found vertical rates of landform transformation on the upper-proximal moraine slope averaged $\sim 0.2 \text{ m yr}^{-1}$ after considering the level of detection permitted by the DEMs used. In previous work, Betz-Nutz *et al.* (2019) highlighted that vertical erosion rates may vary (e.g. 0.06 to 0.10 m yr^{-1}) on upper gullied sections of lateral moraines. Another remote sensing study, undertaken in the Upper Kauner Valley, Austria, found that average rates of vertical lowering on moraine slopes approached 0.06 m yr^{-1} between 1970 and 2006 (Figure 5 in Altmann *et al.*, 2020). These values are lower than the long-term rate of change calculated in this current study, illustrating that the rapid retreat of ice-proximal moraine slopes during deglaciation is possible at selected sites.

Further analysis of vertical change revealed spatial variability in the rate of landform transformation in the upper moraine ice-proximal slope. Here the inter-gully slopes separating gullies were subject to higher rates of denudation (lowering), averaging 0.31 m yr^{-1} in comparison to the gullies (Figure 5D) which experienced, on average, lowering rates of 0.13 m yr^{-1} . This rate of gully erosion compares favourably with long-term rates of gully erosion derived from various studies undertaken at glacier forelands, including those in Norway, where maximum erosion rates of 0.17 m yr^{-1} have been calculated using the volumes of sediment removed from gullies (Curry *et al.*, 2006; Ballantyne, 2002; Benn and Ballantyne, 1994).

The reason for this discrepancy between inter-gully slopes and gullies is likely to relate to the progression of paraglacial slope stabilisation. The *Dufour* Topographic Map of Switzerland (ca. 1861) depicts Glacier d'Arolla occupying the moraine slope, followed by a period of glacier down-wastage noted in the Siegfried 1:50,000

scale maps (Freudiger *et al.*, 2018). By 1977 this down-wastage exposed the moraine slope, resulting in its dissection by well-developed gullies. As these gullies formed, topographically prominent inter-gully slopes developed, leaving them prone to instability by lateral gully extension, and therefore subject to high rates of geomorphological activity. By 2009 a reduction in the depth of these features signified a shift towards greater stabilisation (Figure 5d) (also see Curry *et al.*, 2006). This is supported by the variability in the rate of erosion varying not only in space, but also over time. Here, both rates of change in the gullies and the promontory inter-gully slopes are recorded to slow over time in the upper-proximal zone of the landform (Figures 5a-b).

These findings conform with our existing understanding of paraglaciation, that as time commences from initial glacier recession slopes become increasingly stable (Ballantyne, 2002). For example, in another photogrammetric study by Schiefer and Gilbert (2007) a similar pattern of change over time was observed. Furthermore, “aretes” of *in-situ* diamicton on sediment-mantled slopes have been described by Ballantyne and Benn (1994). This study reveals new details on the morphodynamics of these topographically prominent inter-gully slopes; features that have not previously been widely investigated in Alpine sites using modern landform change detection approaches. The emergence and degradation of *in-situ* till of this nature is perhaps less well studied. Insights from this study should therefore be integrated into models of paraglacial stabilisation of moraine slopes in high-mountain settings. It should, however, be noted that the morphodynamics of moraine slopes have been found to not readily correlate with the time of deglaciation, with the response of lateral moraine slopes to deglaciation suggested to vary at the site level (Betz-Nutz *et al.*, 2023). This diversity in the response and speed of moraine stabilisation makes estimating the precise date of landform stabilisation difficult, and this matter is further complicated by the complex interaction with colonising vegetation in Alpine environments (Eichel *et al.*, 2016).

In summary, landform development at this site appears to follow an expected temporal trajectory, with paraglacial adjustment still in progress. This includes: (1)

the initial onset of gullying upon down-wastage of the glacier and associated loss of ice-support (post-1850s); (2) a period of rapid gully incision on the exposed ice-proximal slopes; (3) the subsequent denudation of well-developed inter-gully slopes (Figure 4); and (4) the future and anticipated onset of stabilisation associated with the “biogeomorphologic feedback window” as discussed in Eichel *et al.* (2016).

Potential implications for palaeo-glaciological studies

The findings of this study have important implications when considering the use of the landform record in palaeo-glaciological studies. The historical extent of glaciers during the Little Ice Age in the Alps is well documented in maps (Freudiger *et al.*, 2018), imagery (Mannerfelt *et al.*, 2023; Mertes *et al.*, 2017; Mölg and Bolch, 2017), and artwork (Zumbühl & Nussbaumer, 2018; Lüthi, 2014; Zumbühl *et al.*, 2008). For areas with more limited records of glacier change over the Holocene and earlier, moraines and trimlines may provide evidence of the former geometry of topographically constrained glaciers (Rootes & Clark, 2020). In the high-Arctic, lateral moraines undergo significant changes in elevation during deglaciation. For example, the work of Midgley *et al.* (2018) indicates lowering of lateral moraines in this setting can exceed $\sim 0.6 \text{ m yr}^{-1}$. This is expected given the ice-cored component of these high-Arctic landforms. However, in alpine settings, where the internal composition of moraines predominately comprises stacked units of diamicton (Small *et al.*, 1984; Humlum, 1978), the significant transformation of lateral moraines is less likely to occur, but as documented here, is possible.

The removal of moraines by slope processes (“external censoring”) may be problematic as the practice of palaeoglacier reconstruction benefits from complete moraine assemblages, which are often used to calibrate the lateral and vertical extent of former glacier models (e.g. Benn & Hulton, 2010; Ng *et al.*, 2010; Pellitero *et al.*, 2015, 2016). Here, it is highlighted that it is not only high-Arctic moraines that are considerably altered during deglaciation (e.g. Ewertowski *et al.*, 2019; Midgley *et al.*, 2018; Tonkin *et al.*, 2016), but that vertical and lateral changes in-excess of 10 metres may also be anticipated in selected alpine settings.

Further work investigating the significance of rapid landform transformation on uncertainty in palaeo-glacier reconstructions may be prudent.

Finally, a robust understanding of moraine degradation is important when considering the correction of Terrestrial Cosmogenic Nuclide dates that may be impacted by boulder exhumation (Heyman *et al.*, 2016). Ice-proximal moraine slopes that have been subject to reworking during deglaciation therefore represent an additional source of uncertainty for the Terrestrial Cosmogenic Nuclide dating of glacial landforms (Kirkbride & Winkler, 2012). In certain settings there may not be a penalty for sampling material for Terrestrial Cosmogenic Nuclide dating from ice-proximal moraine slopes (Tomkins *et al.*, 2021). In Alpine and other high-Mountain settings gullying processes may be active on ice proximal moraine slopes during deglaciation (e.g. Curry *et al.*, 2009), and the modification of proximal slope form and reworking of glacial sediment should be anticipated. Remobilisation of primary sources of glaciogenic sediment through the paraglacial sediment cascade merits consideration for sample selection, especially if the likelihood for previous ice-promixal slope adjustment or failure can be confirmed via sedimentological investigation (e.g. Curry & Ballantyne, 1999).

Conclusion

This study documents the paraglacial adjustment of a lateral moraine from 1977 to 2009. The findings of this study are threefold:

1. The upper gullied lateral moraine slopes at the Bas Glacier d'Arolla were found to have undergone an average depth of surface lowering of 7.15 ± 1.83 m (thresholded) over the observation period (1977 – 2009) corresponding to an average rate of vertical lowering of ~ 0.2 m yr⁻¹. The rate of lowering was, however, found to slow between epochs. The average rate of surface lowering on both, gullies and inter-gully slopes was found to significantly differ between E_1 and E_2 .

2. Whilst the initial removal of ice support results in the rapid incision of ice-proximal slopes by gullying, rapid erosion of inter-gully slopes occurs following gully development. Moreover, rates of erosion on inter-gully slopes were found to significantly exceed gully erosion in both of the observation epochs.
3. Moraine crestlines in steep alpine catchments can rapidly recede and be removed from valley sides by slope processes. Rates of change between ~7 and 15 m over the observation period were detected, yielding an average rate of crestline retreat of 0.34 m yr^{-1} over the 32-year observation period.

Acknowledgments

Financial support provided the British Society for Geomorphology's Early Career Researcher fund enabled the completion of this project. I would like to express my gratitude to anonymous reviewers for their valuable comments on an earlier version of this work.

Data availability statement

The data that support the findings of this study are available from the corresponding author upon reasonable request.

References

- Altmann, M., Piermattei, L., Haas, F., Heckmann, T., Fleischer, F., Rom, J., Betz-Nutz, S., Knoflach, B., Müller, S., Ramskogler, K., & Pfeiffer, M. (2020). Long-term changes of morphodynamics on little ice age lateral moraines and the resulting sediment transfer into mountain streams in the Upper Kauner Valley, Austria. *Water*, 12(12), 3375.
- Ballantyne, C.K. (2002). Paraglacial geomorphology. *Quaternary Science Reviews*, 21(18–19), 1935–2017.
- Ballantyne, C. K., & Benn, D.I. (1994). Paraglacial slope adjustment and re-sedimentation following glacier retreat, Fåbergstølsdalen, Norway. *Arctic & Alpine Research*, 26(3), 255–269.
- Barr, I. D., & Lovell, H. (2014). A review of topographic controls on moraine distribution. *Geomorphology*, 226, 44–64.
- Bennett, G. L., & Evans, D. J. A. (2012). Glacier retreat and landform production on an overdeepened glacier foreland: The debris-charged glacial landsystem at Kvíárjökull, Iceland. *Earth Surface Processes and Landforms*, 37(15), 1584–1602.
- Benn, D. I., & Hulton, N. R. (2010). An Excel™ spreadsheet program for reconstructing the surface profile of former mountain glaciers and ice caps. *Computers & Geosciences*, 36(5), 605–610.
- Benn, D. I., Kirkbride, M. P., Owen, L. A., & Brazier, V. (2003). Glaciated valley landsystems. In D. J. A. Evans (Ed.), *Glacial Landsystems* (pp. 372–406). Oxford University press.
- Betz-Nutz, S., Croce, V., & Becht, M. (2019). Investigating morphodynamics on little ice age lateral moraines in the Italian Alps using archival aerial photogrammetry and airborne LiDAR data. *Zeitschrift für Geomorphologie*, 62(3), 231–247.

Betz-Nutz, S., Heckmann, T., Haas, F., & Becht, M. (2023). Development of the morphodynamics on little ice age lateral moraines in 10 glacier forefields of the Eastern Alps since the 1950s. *Earth Surface Dynamics*, 11(2), 203–226.

Blair, R. W., Jr. (1994). Moraine and valley wall collapse due to rapid deglaciation in Mount Cook National Park, New Zealand. *Mountain Research and Development*, 14(4), 347–358.

Brasington, J., Langham, J., & Rumsby, B. (2003). Methodological sensitivity of morphometric estimates of coarse fluvial sediment transport. *Geomorphology*, 53(3–4), 299–316.

Chandler, B. M., Evans, D. J., Chandler, S. J., Ewertowski, M. W., Lovell, H., Roberts, D. H., Schaefer, M., & Tomczyk, A. M. (2020). The glacial landsystem of Fjallsjökull, Iceland: Spatial and temporal evolution of process-form regimes at an active temperate glacier. *Geomorphology*, 361, 107192.

Cody, E., Anderson, B. M., McColl, S. T., Fuller, I. C., & Purdie, H. L. (2020). Paraglacial adjustment of sediment slopes during and immediately after glacial debuitressing. *Geomorphology*, 371, 107411.

Conrad, O., Bechtel, B., Bock, M., Dietrich, H., Fischer, E., Gerlitz, L., Wehberg, J., Wichmann, V., & Böhner, J. (2015). System for automated geoscientific analyses (SAGA) v. 2.1. 4. *Geoscientific Model Development*, 8(7), 1991–2007.

Curry, A. M., & Ballantyne, C. K. (1999). Paraglacial modification of glacial sediment. *Geografiska Annaler, Series A: Physical Geography*, 81(3), 409–419.

Curry, A. M., Cleasby, V., & Zukowskyj, P. (2006). Paraglacial response of steep, sediment-mantled slopes to post-‘Little Ice Age’ glacier recession in the central Swiss Alps. *Journal of Quaternary Science: Published for the Quaternary Research Association*, 21(3), 211–225.

Curry, A. M., Sands, T. B., & Porter, P. R. (2009). Geotechnical controls on a steep lateral moraine undergoing paraglacial slope adjustment. *Geological Society, London, Special Publications*, 320(1), 181–197.

DiFrancesco, P. M., Bonneau, D., & Hutchinson, D. J. (2020). The implications of M3C2 projection diameter on 3D semi-automated rockfall extraction from sequential terrestrial laser scanning point clouds. *Remote Sensing*, 12(11), 1885.

Draebing, D., & Eichel, J. (2018). Divergence, convergence, and path dependency of paraglacial adjustment of alpine lateral moraine slopes. *Land Degradation & Development*, 29(6), 1979–1990.

Dusik, J-M., Neugirg, F., Haas, F. (2019). Slope wash, gully erosion and debris flows on lateral moraines in the Upper Kaunertal, Austria In: T. Heckmann & D. Morche (Eds.) *Geomorphology of Proglacial Systems*, Cham: Springer, 77–196.

Eichel, J. (2019). Vegetation succession and biogeomorphic interactions in glacier forelands. In T. Heckmann & D. Morche (Eds.), *Geomorphology of Proglacial Systems* Cham: Springer, 327–349).

Eichel, J., Corenblit, D., & Dikau, R. (2016). Conditions for feedbacks between geomorphic and vegetation dynamics on lateral moraine slopes: A biogeomorphic feedback window. *Earth Surface Processes and Landforms*, 41(3), 406–419.

Ewertowski, M. W., Evans, D. J., Roberts, D. H., Tomczyk, A. M., Ewertowski, W., & Pleksot, K. (2019). Quantification of historical landscape change on the foreland of a receding polythermal glacier, Hørbyebreen, Svalbard. *Geomorphology*, 325, 40–54.

Ewertowski, M. W., & Tomczyk, A. M. (2020). Reactivation of temporarily stabilized ice-cored moraines in front of polythermal glaciers: Gravitational mass movements as the most important geomorphological agents for the redistribution of

sediments (a case study from Ebbabreen and Ragnarbreen, Svalbard). *Geomorphology*, 350, 106952.

Freudiger, D., Mennekes, D., Seibert, J., & Weiler, M. (2018). Historical glacier outlines from digitized topographic maps of the swiss alps. *Earth System Science Data*, 10(2), 805–814.

GLAMOS. (2022). Swiss Glacier Length Change, release 2022. *Glacier Monitoring Switzerland*. <https://doi.org/10.18750/lengthchange.2022.r2022>.

Goodsell, B., Hambrey, M. J., & Glasser, N. F. (2002). Formation of band ogives and associated structures at bas glacier d’Arolla, Valais, Switzerland. *Journal of Glaciology*, 48(161), 287–300. <https://doi.org/10.3189/172756502781831494>

Haefeli, R. (1951). Some observations on glacier flow. *Journal of Glaciology*, 1(9), 496–500. <https://doi.org/10.3189/S0022143000026514>

Heyman, J., Applegate, P.J., Blomdin, R., Gribenski, N., Harbor, J.M., & Stroeven, A.P. (2016). Boulder height–exposure age relationships from a global glacial ¹⁰Be compilation. *Quaternary Geochronology*, 34, 1–11.

Heyman, J., Stroeven, A. P., Harbor, J. M., & Caffee, M. W. (2011). Too young or too old: Evaluating cosmogenic exposure dating based on an analysis of compiled boulder exposure ages. *Earth and Planetary Science Letters*, 302(1–2), 71–80.

Humlum, O. (1978). Genesis of layered lateral moraines: Implications for palaeoclimatology, and Lichenometry. *Geografisk Tidsskrift*, 77(1), 65–72.

James, M. R., Robson, S., & Smith, M. W. (2017). 3-D uncertainty-based topographic change detection with structure-from-motion photogrammetry: Precision maps for ground control and directly georeferenced surveys. *Earth Surface Processes and Landforms*, 42(12), 1769–1788.

Kirkbride, M. P., & Winkler, S. (2012). Correlation of late quaternary moraines: Impact of climate variability, glacier response, and chronological resolution. *Quaternary Science Reviews*, 46, 1–29.

Lague D, Brodu N and Leroux J. (2013). Accurate 3D comparison of complex topography with terrestrial laser scanner: Application to the Rangitikei canyon (N-Z). *ISPRS Journal of Photogrammetry and Remote Sensing*, 82 10–26.

Lambiel, C., Maillard, B., Kummert, M., & Reynard, E. (2016). Geomorphology of the Hérens valley (Swiss Alps). *Journal of Maps*, 12(1), 160–172.

Lukas, S., Graf, A., Coray, S., & Schlüchter, C. (2012). Genesis, stability and preservation potential of large lateral moraines of Alpine valley glaciers – towards a unifying theory based on Findelengletscher, Switzerland. *Quaternary Science Reviews*, 38, 27–48.

Lüthi, M. P. (2014). Little Ice Age climate reconstruction from ensemble reanalysis of Alpine glacier fluctuations. *The Cryosphere*, 8(2), 639–650.

Mannerfelt, E.S., Dehecq, A., Hugonnet, R., Hodel, E., Huss, M., Bauder, A., & Farinotti, D. (2023). Halving of Swiss glacier volume since 1931 observed from terrestrial image photogrammetry. *The Cryosphere*, 16(8), 3249–3268.

Mertes, J. R., Gulley, J. D., Benn, D. I., Thompson, S. S., & Nicholson, L. I. (2017). Using structure-from-motion to create glacier DEMs and orthoimagery from historical terrestrial and oblique aerial imagery. *Earth Surface Processes and Landforms*, 42(14), 2350–2364.

Micheletti, N., Lane, S. N., & Chandler, J. H. (2015). Application of archival aerial photogrammetry to quantify climate forcing of alpine landscapes. *Photogrammetric Record*, 30(150), 143–165.

- Midgley, N. G., & Tonkin, T. N. (2017). Reconstruction of former glacier surface topography from archive oblique aerial images. *Geomorphology*, 282, 18–26.
- Midgley N, Tonkin T, Graham D and Cook S. (2018). Evolution of high-Arctic glacial landforms during deglaciation. *Geomorphology*, 311 63–75.
- Mölg N and Bolch T. (2017). Structure-from-Motion Using Historical Aerial Images to Analyse Changes in Glacier Surface Elevation. *Remote Sensing*, 9(10), 1021.
- Ng, F. S., Barr, I. D., & Clark, C. D. (2010). Using the surface profiles of modern ice masses to inform palaeo-glacier reconstructions. *Quaternary Science Reviews*, 29(23–24), 3240–3255.
- Pellitero, R., Rea, B.R., Spagnolo, M., Bakke, J., Hughes, P., Ivy-Ochs, S., Lukas, S., & Ribolini, A. (2015). A GIS tool for automatic calculation of glacier equilibrium-line altitudes. *Computers & Geosciences*, 82, 55–62.
- Pellitero, R., Rea, B.R., Spagnolo, M., Bakke, J., Ivy-Ochs, S., Frew, C. R., Hughes, P., Ribolini, A., Lukas, S., & Renssen, H. (2016). GlaRe, a GIS tool to reconstruct the 3D surface of palaeoglaciers. *Computers & Geosciences*, 94, 77–85.
- Putkonen, J., & Swanson, T. (2003). Accuracy of cosmogenic ages for moraines. *Quaternary Research*, 59(2), 255–261.
- Rootes, C. M., & Clark, C. D. (2020). Glacial trimlines to identify former ice margins and subglacial thermal boundaries: A review and classification scheme for trimline expression. *Earth-Science Reviews*, 210, 103355.
- Röthlisberger, F., & Schneebeli, W. (1979). Genesis of lateral moraine complexes, demonstrated by fossil soils and trunks: Indicators of postglacial climatic fluctuations. In C. Schlüchter (Ed.), *Moraines and varves*, Rotterdam: Balkema (pp. 387–419).

Schiefer, E., & Gilbert, R. (2007). Reconstructing morphometric change in a proglacial landscape using historical aerial photography and automated DEM generation. *Geomorphology*, 88(1–2), 167–178.

Schimmelpfennig, I., Schaefer, J.M., Akçar, N., Ivy-Ochs, S., Finkel, R.C., & Schlüchter, C. (2012). Holocene glacier culminations in the Western Alps and their hemispheric relevance. *Geology*, 40(10), 891–894.

Small, R. J. (1983). Lateral moraines of glacier de tsidjiore Nouve: Form, development and implications. *Journal of Glaciology*, 29(102), 250–259.

Small, R. J., Beecroft, I. R., & Stirling, D. M. (1984). Rates of deposition on lateral moraine embankments, glacier de tsidjiore Nouve, Valais, Switzerland. *Journal of Glaciology*, 30(106), 275–281.

SwissTopo. (2019). *swissALTI3D - Rapport sur la publication 2019*. Federal Office of Topography.

Tomkins, M.D., Dortch, J.M., Hughes, P.D., Huck, J.J., Pallàs, R., Rodés, Á., Allard, J.L., Stimson, A.G., Bourlès, D., Rinterknecht, V., & Jomelli, V. (2021). Moraine crest or slope: An analysis of the effects of boulder position on cosmogenic exposure age. *Earth and Planetary Science Letters*, 570, 117092.

Tonkin, T. N., Midgley, N. G., Cook, S. J., & Graham, D. J. (2016). Ice-cored moraine degradation mapped and quantified using an unmanned aerial vehicle: A case study from a polythermal glacier in Svalbard. *Geomorphology*, 258, 1–10.

van Woerkom, T., Steiner, J. F., Kraaijenbrink, P. D., Miles, E. S., & Immerzeel, W. W. (2019). Sediment supply from lateral moraines to a debris-covered glacier in the Himalaya. *Earth Surface Dynamics*, 7(2), 411–427.

Warburton, J. (1994). Channel change in relation to meltwater flooding, Bas Glacier d’Arolla, Switzerland. *Geomorphology*, 11(2), 141–149.

Warburton, J., & Beecroft, I. (1993). Use of meltwater stream material loads in the estimation of glacial erosion rates. *Zeitschrift für Geomorphologie*, 37(1), 19–28.

Warburton, J., & Fenn, C. R. (1994). Unusual flood events from an Alpine glacier: Observations and deductions on generating mechanisms. *Journal of Glaciology*, 40(134), 176–186.

Westoby, M., Brasington, J., Glasser, N. F., Hambrey, M. J., & Reynolds, M. J. (2012). Structure-from-Motion photogrammetry: A low-cost, effective tool for geoscience applications. *Geomorphology*, 179, 300–314.

Wheaton, J. M., Brasington, J., Darby, S. E., & Sear, D. A. (2010). Accounting for uncertainty in DEMs from repeat topographic surveys: Improved sediment budgets. *Earth Surface Processes and Landforms*, 35(2), 136–156.

Winiwarter, L., Anders, K., & Höfle, B. (2021). M3C2-EP: Pushing the limits of 3D topographic point cloud change detection by error propagation. *Isprs Journal of Photogrammetry & Remote Sensing*, 178, 240–258.

Zumbühl, H. J., & Nussbaumer, S. U. (2018). Little ice age glacier history of the central and Western Alps from pictorial documents. *Cuadernos de Investigación Geográfica*, 44(1), 115–136.

Zumbühl, H. J., Steiner, D., & Nussbaumer, S. U. (2008). 19th century glacier representations and fluctuations in the central and western European Alps: An interdisciplinary approach. *Global and Planetary Change*, 60(1–2), 42–57.

Figure captions

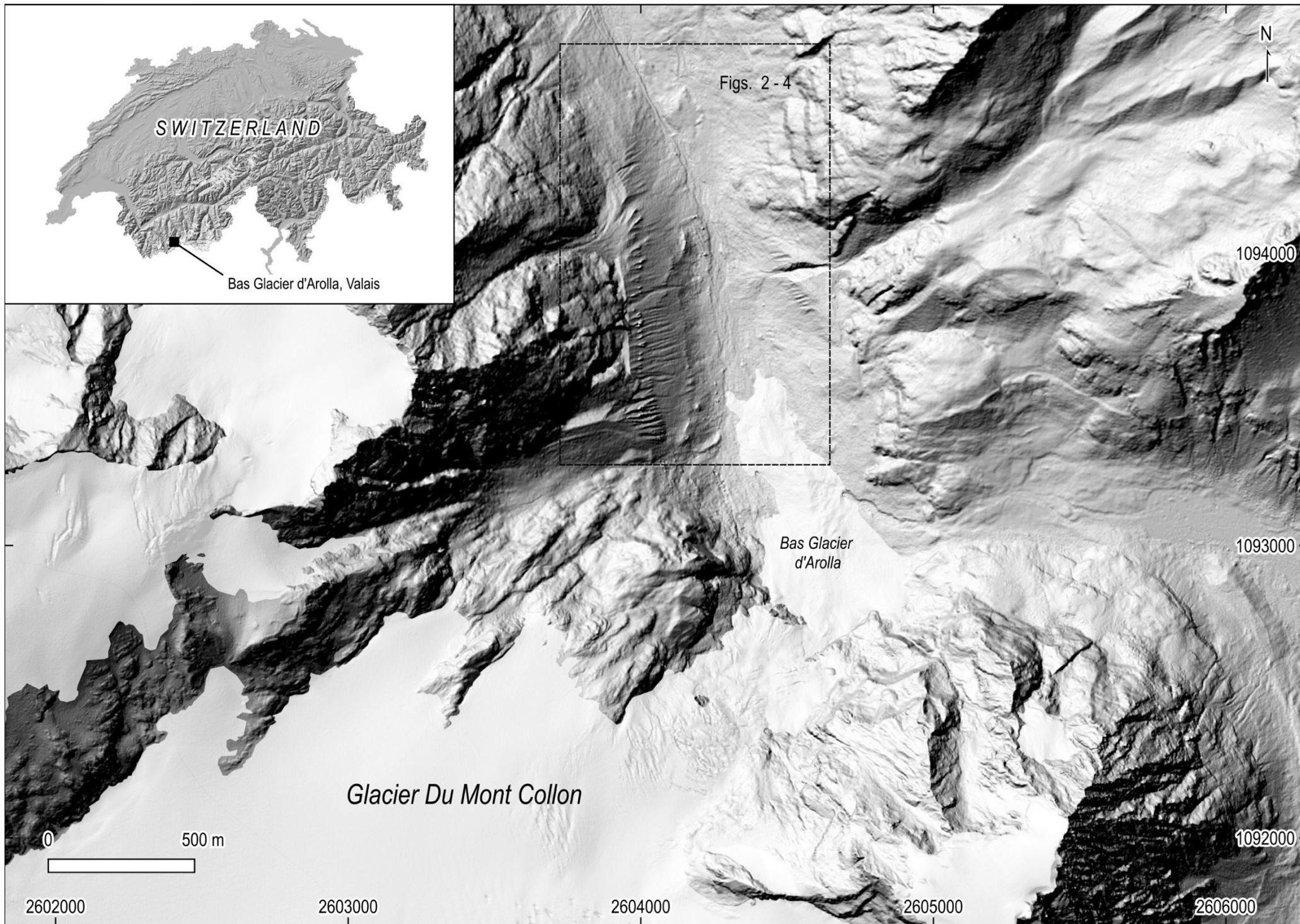
Figure 1. A SwissAlti^{3D} hillshaded digital elevation model of the study area (2019). The image covers the Western branch of the Val d'Herons and the Bas Glacier d'Arolla (Federal Office of Topography, © swisstopo).

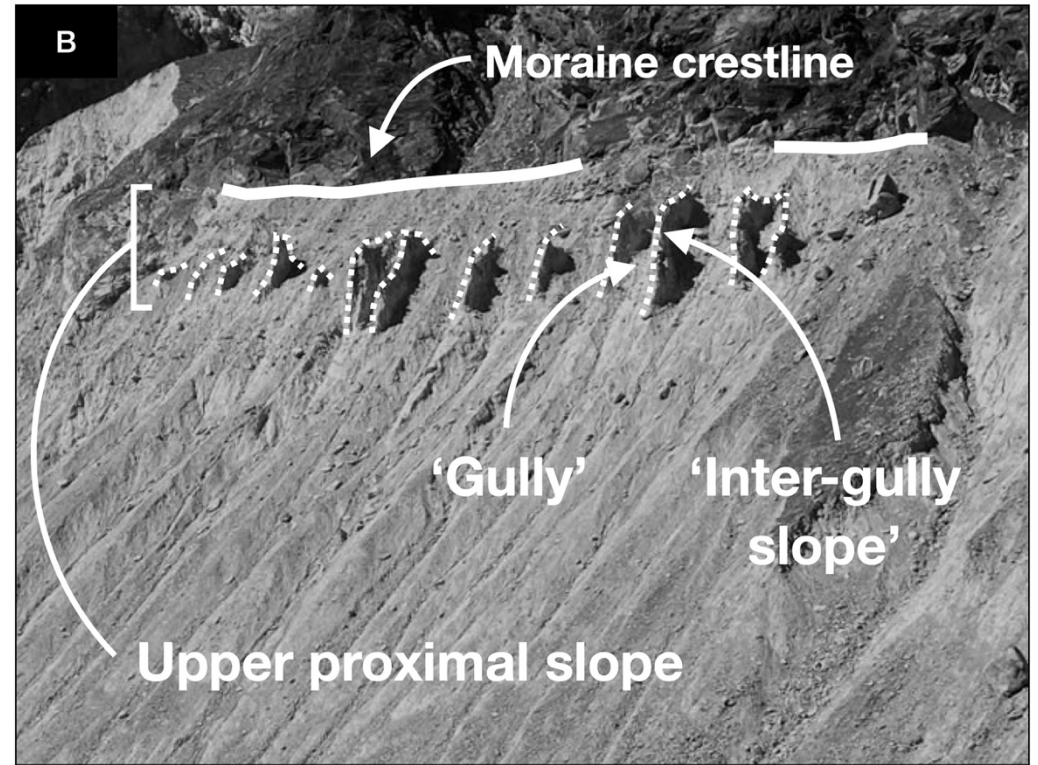
Figure 2. The landform elements referred to in this study. (A) An oblique overview of the study site in August 2022 as viewed when looking southwest from the adjacent valley-wall. (B) An annotated diagram of the landform elements and upper-proximal zone of the landform.

Figure 3. The Digital Elevation Models of Difference (DoD) covering E_1 (1977–1988) and E_2 (1988–2009) as generated by this study. Note the glacier advance in E_1 (positive elevation change in panel a) and recession in E_2 (negative elevation change in panel b). The orthoimagery in panel (a) was produced using the 1988 image set. The orthoimagery displayed in panel (b) is derived from the 2009 image set.

Figure 4. Cloud to Cloud differencing over E_d (1977–2009). The two hillshaded panels (top left) highlight the changes to gullies and the associated inter-gully slopes over the study period. The elevation data shown here were generated by this study using the archive 1977 and 2009 image sets. Profile $i - i'$ can be seen in the bottom left corner. Profile $D - D'$ is displayed in Figure 5.

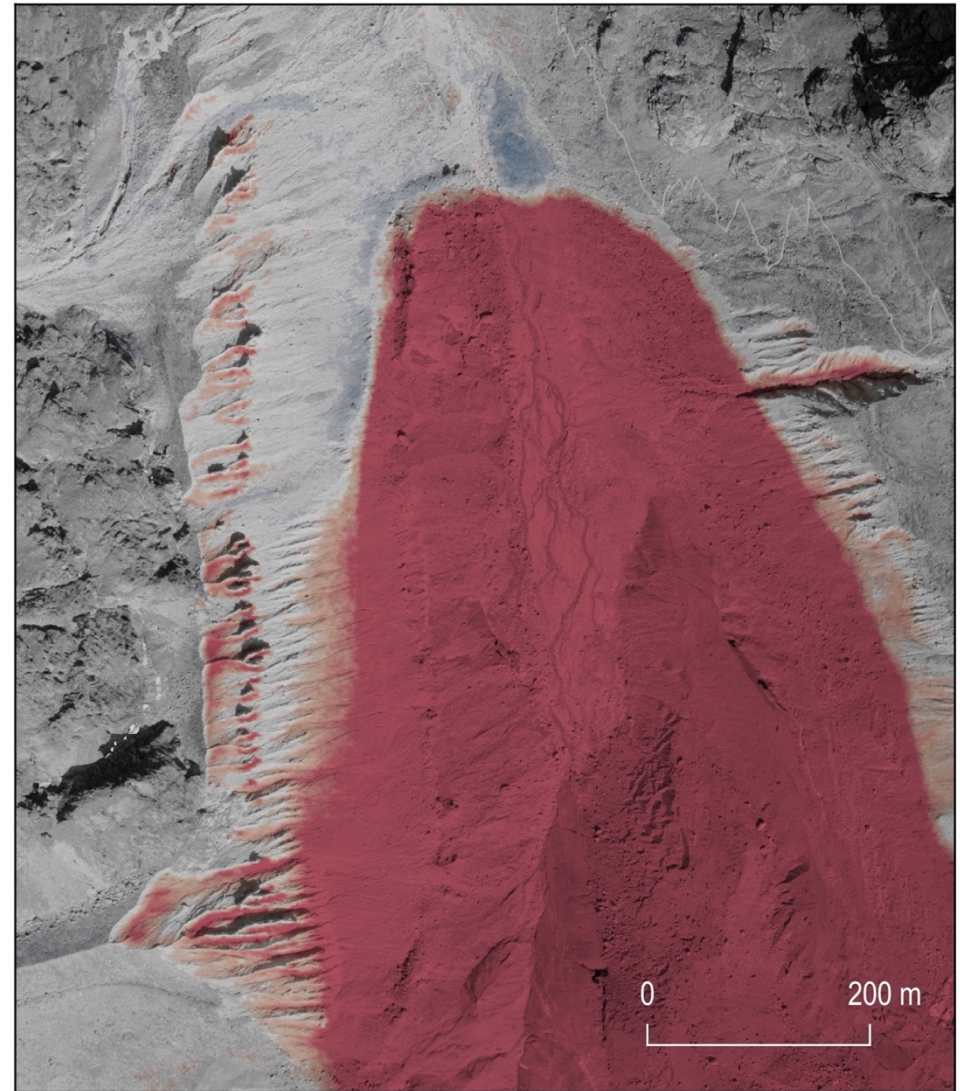
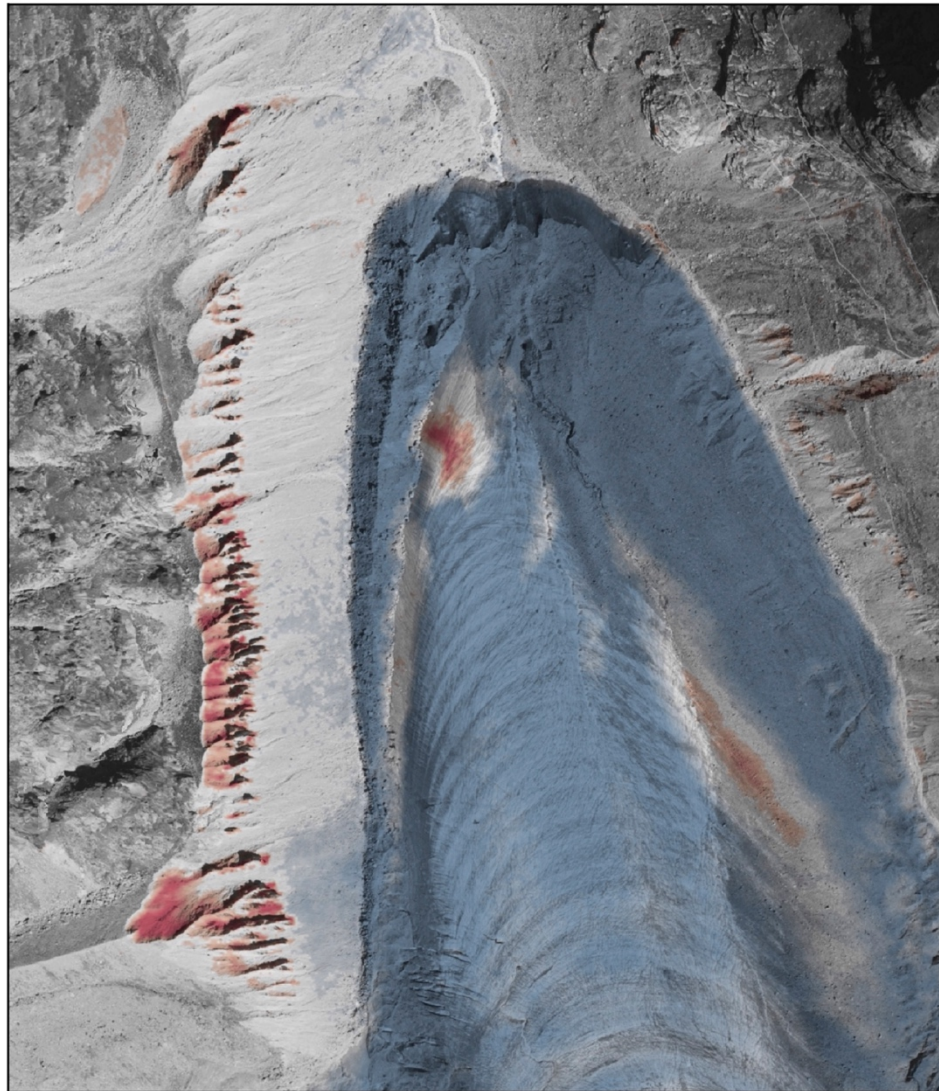
Figure 5. Comparisons of geomorphological change between epochs and landform elements. (A) The average rate of vertical change in gully and gully-like features between E_1 and E_2 . (B) The average rate of vertical change for the inter-gully features separating prominent gullies between E_1 and E_2 . (C) A comparison of the vertical rate of change over the observation period (E_d) for both landform elements. (D) A topographic profile with the measurement locations annotated.

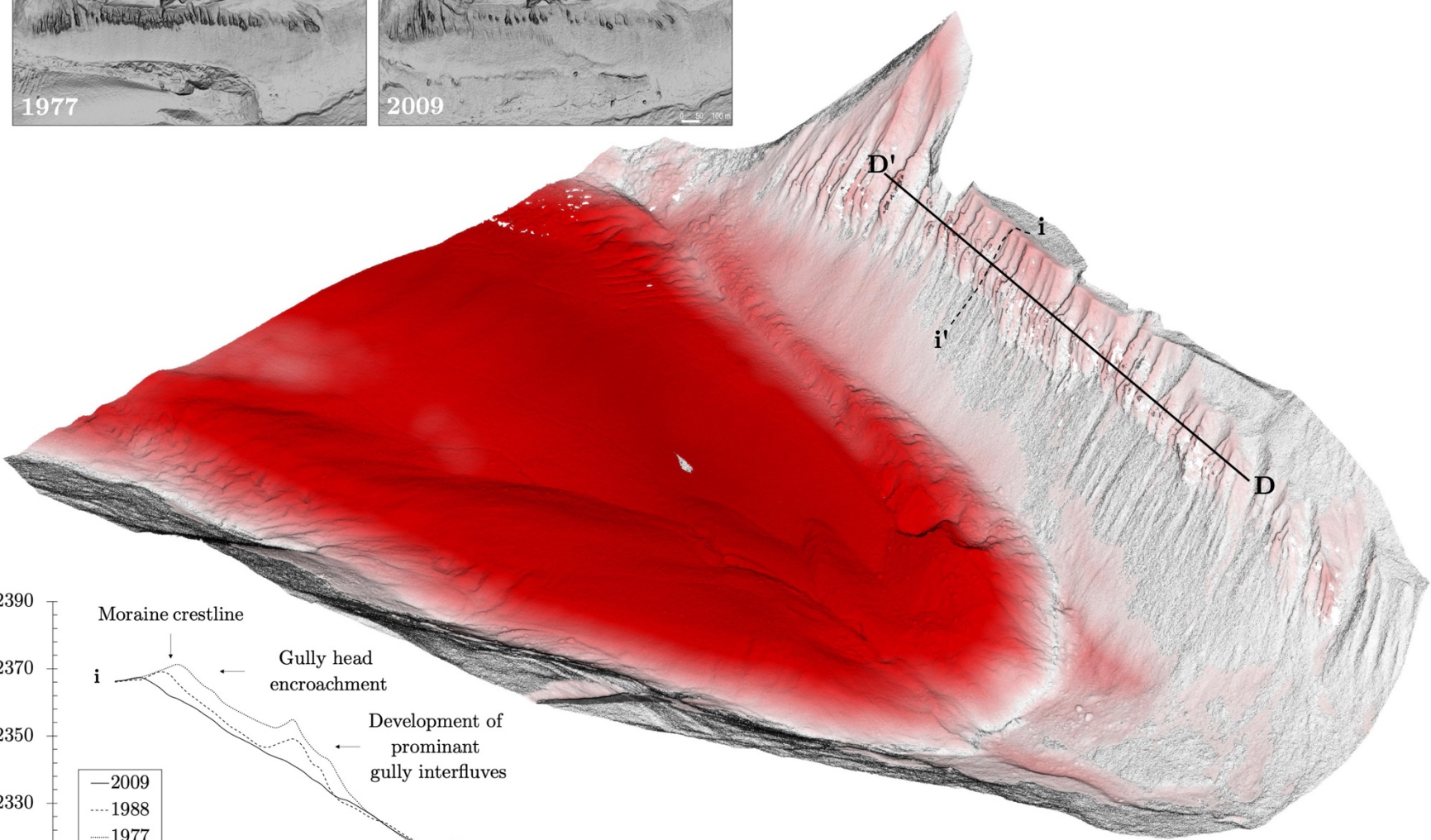
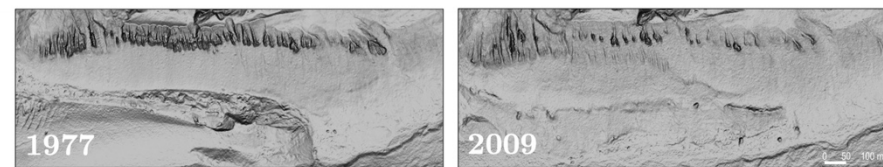




(a) 14.09.1977 to 09.08.1988 (LoD₉₅ = 2.71 m)

(b) 09.08.1988 to 07.09.2009 (LoD₉₅ = 2.43 m)





C2C absolute distances

